https://ntrs.nasa.gov/search.jsp?R=19780004587 2020-03-22T06:55:54+00:00Z

Casefile Copy

N78-12530

NASA Contractor Report 145268

OPTIMIZATION OF SOLAR CELLS FOR AIR MASS ZERO OPERATION AND A STUDY OF SOLAR CELLS AT HIGH TEMPERATURES

Final Report - Phase III

A. E. Blakeslee, H. J. Hovel and J. M. Woodall

NASA Contract NASI-12812

NASA Contractor Report 145268

OPTIMIZATION OF SOLAR CELLS FOR AIR MASS ZERO OPERATION AND A STUDY OF SOLAR CELLS AT HIGH TEMPERATURES

Final Report - Phase III

A. E. Blakeslee, H. J. Hovel and J. M. Woodall

NASA Contract NASI-12812

NASA

National Aeronautics and
Space Administration

OPTIMIZATION OF SOLAR CELLS FOR AIR MASS ZERO OPERATION AND A STUDY OF SOLAR CELLS AT HIGH TEMPERATURES

A. E. Blakeslee, H. J. Hovel and J. M. Woodall

IBM Thomas J. Watson Research Center

P. O. Box 218

Yorktown Heights, New York 10598

I. Objective

The purpose of this contract is to develop crystal growth procedures, fabrication techniques, and theoretical analyses in order to make GaAlAs-GaAs solar cell structures which exhibit high performance at: 1)Air Mass 0 illumination and 2)high temperature conditions.

II. Introduction

The work described in this report is part of an on-going effort over the last three years to optimize the behavior of GaAs solar cells for AM0 operation. The efficiencies of these cells have climbed steadily from the 13-14% value (contact area corrected) reported at the end of Phase I to the 18.5% (uncorrected for contact area) value reported in the middle of the present Phase III. The improvement has been brought about by a combination of changes in the liquid phase epitaxial (LPE) growth technique that have resulted in thinner GaAlAs layers, the development of a leaching step to improve the diffusion length in the starting substrate, and the development of contact metallurgies which obviate the extra Zn diffusion step.

This report will begin with a description of the "etch-back epitaxy" process for producing thin, graded composition GaAlAs layers. In the second section, the palladium-aluminum contact system is discussed along with its associated problems. Recent solar cell results under simulated AM0 light and at elevated temperatures are described in the third section, and in the final section, the growth of thin polycrystalline GaAs films on foreign substrates is described.

III. Liquid Phase Epitaxial Growth Studies

During this phase several important developments were made in the LPE growth procedures which resulted in greatly improved solar cell efficiency. Previous attempts to grow p-type $Ga_{.1}Al_{.9}As$ layers $\approx$ 0.5 μ thick by the normal procedure of "gettering" the n-type GaAs substrate in an equilibrium Ga-Al-As Zn doped melt followed by a shortened ramp cooling schedule usually resulted non-uniform coverage of the GaAs substrate by the $Ga_{1-x}Al_xAs$ layer. Experiments in which ramp cooling was initiated prior to substrate-melt contact produced more uniform coverage; however, the resulting cells exhibited very poor minority carrier diffusion lengths. This is consistent with the observation that substrate-melt contact prior to growth for a sufficient time (usually greater than five minutes) results in improved minority carrier diffusion lengths in both the p and n type regions of the substrate after growth. The conclusion was that gettering prior to growth was necessary for good diffusion lengths, but that ramp cooling prior to melt-substrate contact was necessary for the growth of 0.5 μ thick uniform layers of $Ga_{1-x}Al_xAs$. These seemingly conflicting requirements were resolved by the development of a novel growth method called etchback-regrowth epitaxy. Basically, this technique involves bringing a GaAs n-type substrate in contact with an undersaturated melt of Ga-Al-As doped with Zn. An undersaturated melt is capable of dissolving more Al or As or both until solid-liquid equilibrium is reached. Upon contact a small amount of the GaAs wafer dissolves. Since the melt is basically stagnant, the melt forming near the solid liquid interface is richer in Ga and As than the bulk of the melt producing a diffusion couple. As diffusion proceeds, the melt next to the solid-liquid interface at first becomes saturated, which stops the etching of the GaAs substrate, and then becomes supersaturated which causes the regrowth of a thin (0.2-0.4 μ thick) $Ga_{1-x}Al_xAs$ p-type layer graded in composition from x=0 at the interface to an x value corresponding to liquid-solid equilibrium value, usually 0.9-0.95 for these studies.

The etchback-regrowth experiments can be summarized by the growth schedules in Figs. 1 and 2. In Fig. 1, the Ga-Al Zn doped melt is saturated isothermally with As via

contact with an excess of GaAs. After equilibrium, the excess GaAs is removed and the temperature of the melt raised 10-20°C followed by substrate-melt contact for 10-60 minutes. Then the substrate and regrowth is separated from the melt. The temperature range studied for this schedule was 850°-900°C. In the schedule of Fig. 2, the GaAs substrate provides the As necessary to achieve both saturation and regrowth. The temperature range studied for this schedule was 750-850°C. The apparatus used was of the rotating slides type (Fig. C in Ref. 1). The melt charges were all based on 2.5 gms Ga, and 0.035 gms Al. The Zn doping levels studied were 0.035-0.100 gms.

The metallurgical and device characteristics of the etchback-regrowth structures were studied. The device properties are reported in Section V. It was found that using the growth schedule, Fig. 1, at temperatures between 875 and 900°C produced large decomposition etch pits in the substrate which persisted even after the etchback-regrowth step. These pits, 10-20 μ across, were formed of (III) facets and were sometimes filled with melt after growth. These large pits were found not to affect the spectral response of the cell. However, they drastically lowered the open circuit voltage. It was concluded that the pits caused small areas of low-shunt resistance, perhaps in the form of small area Schottky diodes formed by the melt pit wall interface, in a parallel circuit with normal p-n junction material. This problem was greatly reduced by lowering the temperature to 850°C and shortening the time of wafer surface exposure to a gas ambient prior to melt contact.

Good solar cells (η_{AM0}>15%) can be grown by either growth schedule. For Fig. 1, a melt contact temperature of 800-850°C, a Zn doping of 0.035-0.50 gms and a substract-melt contact time of 10-20 minutes can be used. For Fig. 2, a melt-substrate temperature of 800-835°C, a Zn doping of 0.035-0.050 gms and a melt contact time of 15-30 minutes can be used. For these parameters, the p-n junction depth is 1.5-2.0 μ and the $Ga_{1-x}Al_xAs$ layer thickness is about 0.1-0.3 μ.

IV. Contact Technology

In Section III of the Final Report, Phase II of this contact, the contact resistances of several metal combinations to p-type GaAs and GaAlAs were given. Of the combinations which were tested, including Cr-Au, Al-Mg, Ag-Mg, Cr, Au, and Pd, only palladium was capable of producing a low resistance contact to material of low doping level ($1\text{-}4 \times 10^{18}$ cm^{-3}) without annealing at high temperatures. For this reason, a contact metallurgy of 500 Å Pd followed by 5000 Å of Al was adopted; Al was chosen on the basis that it would not produce doping or shunting effects in the GaAlAs or GaAs during high temperature operation.

The Pd/Al contact is evaporated onto the solar cell surface through a stainless steel mask. The pattern consists of 1 mil-wide lines spaced 30 mils apart and joined by a single 5 mil line running down the middle. The ohmic contact to the bottom nGaAs side of the cell is made with a Sn/In/Ga liquid metal mixture, which produces a low resistance contact without annealing. The finished device is mounted onto a TO-5 or Al header with Ag conducting epoxy, and a wire is bonded to the 5 mil stripe also with Ag epoxy.

This technique was highly reliable in producing solar cells with high open circuit voltages, and allowed short circuit current, open circuit voltage, and spectral response measurements to be made routinely. However, the fill factors were poor due to a high series resistance, generally between 10 and 100 ohms for unannealed cells. Annealing the samples at temperatures of 200-300°C reduced the series resistance to the 3-6 ohm range, but often produced shunt paths which lowered the open circuit voltage. Table 1 shows a good example of this behavior, in which the series resistance and V_{oc} were both initially high. The series resistance of the first device was reduced by a factor of nearly 10 after annealing at 275°C for 10 minutes, but further heat treatment raised the leakage current (measured at -1 volt) and lowered the V_{oc} without improving the series resistance to an acceptable value.

A further problem observed with the Pd/Al Al-contacted samples was an initial very high series resistance (thousands of ohms) when voltage was first applied to the sample. This resistance would switch suddenly to the values of Table 1 when 4 to 5 volts were applied.

The most probable cause of the problem is the native oxide on the Al layer which insulates the grid pattern from the Ag epoxy contact. Destructive breakdown of the oxide takes place when a sufficient field is applied across it, allowing electrical contact to be made to the grid.

A more subtle problem of the Pd/Al system was a tendency in some devices for the series resistance to first decrease with annealing temperature and then increase again for higher temperatures, never reaching an acceptably low value. This might be due to an interdiffusion of the Pd and Al which essentially removes the Pd from the GaAs/metal interface. It is known that Pd and Al form several compounds at low temperatures, so that an actual driving force exists for removing Pd from the interface, leaving an Al/GaAs contact which has a high contact resistance.

For these reasons, it was decided to adopt a Pd/Ag metallurgy in place of Pd/Al. Pd/Ag has been used for Si solar cells very successfully for a number of years (together with Ti) and may not have the interdiffusion problems of the Pd/Al system. In addition, Ag does not form an insulating native oxide, and is easy to contact electrically.

The Pd/Ag combination greatly enhanced the reliability of the ohmic contact to the upper surface. The initial contact resistances were of the order of 15 to 20 ohms, and these were reduced to about 4 ohms after annealing at 250°C. Since the sheet resistivity of the upper p-type layer is about 500 ohms per square and the grid pattern has 13 lines per cm, the calculated sheet resistance of the thin p-type region is about 1 ohm, or one-third to one-fourth of the observed series resistance. The remainder is most likely due to the contact resistance between the Pd and the GaAlAs.

For the sample sizes most commonly used, about 0.2 cm^2, the photocurrent is around 6 milliamps, and the voltage drop for a 4 ohm series resistance is 24 millivolts. This is high enough to reduce the fill factor from an expected 0.82 to about 0.79. Higher temperature annealing may reduce the series resistance further, but may also lead to reduced open circuit voltages if any Ga droplets are left to form shunts across the p-n junction. In the future, finer

grid patterns will be used to reduce the sheet resistance contribution and higher temperature annealing will be explored as a means of reducing the contact resistance portion.

V. Solar Cell Results

A. Spectral Response and Device Behavior

The etchback epitaxy process was developed as a means of obtaining uniform thin GaAlAs layers necessary for high quantum efficiencies and high photocurrents. The GaAlAs layer appears to be graded in composition as well as thin, both of which contribute to high spectral responses at photon energies above 2.5 eV (wavelengths of 5000 Å or less).

The spectral responses of several representative devices grown at 870°C are shown in Fig. 3. These devices are characterized by a nearly flat response for photon energies just above the band gap to about 2.5 eV, followed by a fairly steep decline for higher energies. The Zn concentration in the melt seems to have a significant effect on the response; the higher the Zn level, the sharper the cut-off. This might be due to a smaller diffusion length or higher surface recombination velocity for the GaAlAs, or it could be due to an effect on the GaAlAs layer thickness.

A considerable difference is observed in the responses of cells grown at lower temperatures, as can be seen by comparing the 800°C devices of Fig. 4 with the devices of Fig. 3. At low energies, the response increases with increasing energy, indicating that the leaching effect[2] is not as effective at 800°C as at 870°C. The drop-off in response at high photon energies is gradual, compared to the sharper cut-off for the higher temperature cells. This probably indicates that the GaAlAs is thinner in the low temperature devices.

After the solar cells were mounted on headers, they were covered with a 600-700 Å layer of TiO_2 as an anti-reflective coating. These coatings were prepared by the reactions of the titanium organic compound $Ti\ (OC_3H_7)_4$ and water vapor[3], sprayed onto the devices at a temperature of 140-175°C. The index of refraction under these conditions is around 2.05, which is slightly higher than the ideal index for these cells, but the convenience of the process

is highly advantageous. Figure 5 compares the spectral responses of several devices before and after the TiO_2 is applied. The absolute quantum efficiencies at the peak of the solar spectrum (5500-6000 Å) generally range from 96 to 99%.

The open circuit voltages, short circuit currents, fill factors, and conversion efficiencies under simulated AM0 conditions for several representative devices are given in Table 2. The power input was determined using test cells measured under the AM0 simulator at JPL in Pasadena, California. In almost all cases the photocurrents exceed 30 mA/cm^2, with V_{oc}'s of around a volt. The series resistances and fill factors, however, vary from sample to sample due to the unreliable Pd/Al contact metallurgy. The last two samples were made with the Pd/Ag metallurgy, resulting in considerably improved fill factors. The conversion efficiencies approach or exceed 18% in devices with good fill factors. No corrections have been made for the contact area, which is about 4% of the total surface area.

B. Temperature

Some theoretical calculations and measurements of solar cell behavior as a function of temperature were given in the Phase II final report of this contract. It was shown there that the spectral response shifts to lower energies at higher temperatures due to the shift in bandgap and absorption edge of GaAs. Some improvement occurs in the diffusion length also. These two effects result in an increasing short circuit current with increasing temperature. The dominant effect of temperature, however, is on the open circuit voltage, and the decrease in V_{oc} causes an approximately linear decrease in the efficiency.

Measurements of solar cell behavior as a function of temperature are complicated by the absence of a reliable AM0 light source. Use of the infrared absorbing filter removes most of the light above 8500 Å (see Fig. 6), and the benefits of the shifting GaAs absorption edge are not obtained with the remaining spectrum. On the other hand, the 8500-9000 Å spectral range is greatly exaggerated without this filter, which would lead to an over-estimate of the efficiency as a function of temperature.

During the present phase of the contract, device measurements as a function of temperature were made in two ways: 1)under AM1.5 solar radiation, 2)under simulated AM0 illumination, using the H_2O and I.R. filtered Xe light. The temperature was monitored by a thermocouple attached to the TO-5 header.

The photocurrent as a function of temperature is shown in Fig. 7. The current initially increases with temperature, which is expected from the shift in spectral response (see Final Report, Phase II), but this is followed by a slight decline above several hundred degrees. This decline might be due to a shift in the GaAlAs absorption edge, cutting off an increasing amount of light from reaching the underlying GaAs p-n junction. The open circuit voltage, Fig. 8, follows a well defined linear relationship, as expected from the variation of η_i with temperature[4], and as a result, the efficiency varies linearly with temperature as shown in Fig. 9. The AM0 efficiency is slightly under-estimated due to the infrared filtering.

A number of difficulties were encountered during the measurements for temperatures of 200°C or above. The Pd/Al contact often becomes highly resistive, and could only be made low in resistance again by passage of a high current (several hundred milliamps) through the device. The Ag epoxy became unreliable also, occasionally acting as an open-circuit. Preliminary results with Pd/Ag contacts and solder bonding indicate that these problems can be eliminated.

C. Thin Junction Diffused Cells

A method has been devised to test the "violet" cell principle in GaAs, whereby surface recombination problems are overcome using a very narrow junction (~ 1000 Å). The violet cell design should be even more important in GaAs than in Si because of the greater importance of the regions near the surface in GaAs. The method involves the removal of thin layers of GaAs from the surface in 500 Å steps using anodization. The result is a study of GaAs solar cell for junction depths of 500 Å to 3000 Å. These devices can then be compared with GaAs-GaAlAs cells.

The starting substrate was an n-type GaAs wafer having a 20 μm thick vapor deposited layer doped to $2x10^{17}$ cm^{-3}. The starting hole diffusion length in this layer was 2.0 μm. The wafer was sealed at 10^{-7} Torr in a quartz ampoule of 5 cm^3 volume together with 5 mg of the Zn diffusion source, which consisted of 5% Ga, 50% As, and 45% Zn by weight. The ampoule was placed in a furnace pre-set to 700°C for a period of about two minutes, which resulted in junction depths of about 3000 Å as measured by angle lapping and staining. Ohmic contact to the back was made using Au-Ge-Ni evaporated layers or by applying a Ga-In-Sn liquid alloy. An ohmic contact grid of Al about 2000 Å thick was evaporated onto the diffused p region through a metal mask.

The spectral response, current-voltage behavior, and AM0 efficiency were first measured on the devices as produced above. The cells were then immersed in a water-phosphoric acid solution with a pH of 2 and anodized at a voltage of 40 volts with respect to a Pt cathode. This produced a deep blue anti-reflection coating on the cell and converted about 500 Å of the GaAs surface to an oxide. The solar cell behavior of the device was measured again, and then the anodized layer was removed in a 1:1 mixture of photo-resist developer and water. The surface was then re-anodized, removing another 500 Å layer, and in this way the properties of the cell could be studied as a function of junction depth until the entire junction had been removed. The Al upper contact is essential in this process; other metals are etched away during the anodizing step, but a protective Al_2O_3 layer is formed on the Al surface which prevents contact deterioration.

The spectral responses as a function of junction depth are shown in Fig. 10. Before any anodization, the characteristic triangular-shaped recombination loss is seen. As the junction depth is reduced, the response to high energy (short wavelength) light is improved, but the response is not quite as high as expected from calculations using a 2 μm diffusion length in the base and a junction depth of 1000 Å, shown as a dotted line in Fig. 10. The difference may be due to poor conditions in the diffused region or to absorption in the anodization-produced oxide layer.

The dark current-voltage behavior as a function of junction depth is shown in Fig. 11. The slopes of the ln J-V curves are nearly always around two, indicating dominance by recombination within the depletion region. There is some improvement in the characteristic after anodizing compared to before, possibly due to some passivation of surface states when the anodization oxide is formed around the junction edges.

The short circuit current and AM0 efficiency as a function of junction depth are shown in Fig. 12. The short circuit current reaches about 22 mA/cm^2 for the narrowest junction, with an open circuit voltage of 0.90 volt and a fill factor of 0.70 for an efficiency of 10.3%. The efficiency at AM1 is considerably higher (13-14%) since the device is much more sensitive to 2.0 eV photons than to high energy photons (Fig. 10).

The efficiencies of the best diffused GaAs "violet cells" were about 11% (without contact area correction) using substrates with 3.0 μm starting diffusion lengths. Substrates with smaller diffusion lengths gave considerable lower efficiencies. Even the best diffused violet cells were not nearly as good as typical $Ga_{1-x}Al_xAs$-GaAs cells. The expected strong increase in the photocurrent and efficiency of the diffused cells with decreasing junction depth was not observed; the reason for this is not understood at this time.

VI. Polycrystalline GaAs Films for Photovoltaic Applications

As has been pointed out by Woodall and Hovel[5], GaAs photovoltaic devices could make an impact on large scale terrestrial energy production if their cost could be drastically reduced. There is currently a large effort going on at several academic and industrial institutions which is aimed at trying to bring about such a cost reduction. The major part of this objective is to be accomplished through an approximately 50-to-100-fold reduction in the thickness of the GaAs incorporated in the device. This means that the active layer will be a 2-5-μm layer of n-type polycrystalline GaAs on an inexpensive and readily-available conductive substrate, such as graphite, stainless steel or molybdenum. In addition to the requirement of thinness for the polycrystalline GaAs layer, it is also necessary that the average grain

diameter be at least several microns; that the grain structure be columnar, i.e., that there be essentially no components of the grain boundaries in the film plane; and that the film be continuous. Lanza and Hovel[6] have calculated that 2-μm-thick polycrystalline GaAs films consisting of columnar grains having an average diameter of 3 μm can be fashioned into Schottky-barrier solar cells exhibiting a maximum efficiency of 12%. Poly GaAs cells that were 3-5% efficient were reported by Vohl et al[7] in 1967, but, somewhat curiously, this result has apparently not been reproduced or improved upon since then.

The method chosen for growth of the poly GaAs films is the so-called metal-organic process[8,9] in which $Ga(CH_3)_3$ vapor and AsH_3 gas are reacted to form GaAs on an RF-heated substrate. The metal-organic process is preferred to the close-spaced transport scheme used by Vohl et al[7] in spite of the fact that the latter process has been demonstrated to be capable of producing columnar-grained films yielding reasonably efficient solar cells, while the former has not. The reason is simply that the metal-organic technique is undoubtedly more amenable to conversion to a large-scale manufacturing process, which is, of course, the ultimate objective. Initial conditions of film deposition were chosen to be those which had proved optimum for epitaxial growth of GaAs on GaAs substrates - namely, 700°C and flow rates chosen so as to yield a deposition rate of ~ 0.5 μm/min.

Under such conditions it is no problem to obtain poly films on foreign substrates; our task boiled down in large part to ensuring that these films consisted of large columnar grains. Our first approach to that task was to search for substrates which would induce epitaxial growth and thereby guarantee large grains. This approach appeared promising in view of the reported epitaxial growth of GaAs on W by Amick.[10] Many substrates were tried, ranging in degree of crystallinity from single crystal to amorphous. These included single crystals of Si and W; polycrystalline sheets of W, Mo and Ta; and vitreous silica and carbon. The result in every case was essentially the same. Neither epitaxy nor oriented growth was achieved for any of the substrates.

Figure 13 illustrates the morphology of three typical films grown on three different polycrystalline metal substrates. All three consist of highly faceted, less than 1-μm average diameter grains, with no evidence of texturing. The differences observable among these three examples are not significant; they are attributable to run-to-run variations and to the mode of growth of the films. They do not grow as most polycrystalline films do - namely by forming stable nuclei which then expand coherently, by both surface diffusion and attachment from the fluid phase, until they coalesce and form a continuous film. Instead, a "nodular" form of growth takes place in which the initial small crystal nuclei serve as the starting point for the piling-up of many more similar small crystals. Such microcrystalline nodules expand, coalesce and finally form a rough-surfaced but otherwise uniform film. Traces of these nodules can be seen in Fig. 13. This type of growth obviously gives rise to very many horizontally-oriented grain boundaries, an undesirable situation from the standpoint of solar cell efficiency. Why it is that new grains nucleate on top of existing ones, and why no interfacial coherence was observed with any of the substrates tried, are both puzzling questions in the light of the good results always obtained with GaAs substrates. Perhaps the answers are connected with the fact that the chemistry of the metal-organic system is very different from that of the close-spaced transport method which yielded columnar grains[7] and also that of the chloride transport method which yielded epitaxy of GaAs on W.[10]

Having been unsuccessful in our search for an inexpensive foreign substrate that would induce growth of large GaAs grains, we then turned to the approach of applying special pre- or post-treatments to the substrates or films, as the case may be. Figure 14 illustrates examples of some of these. The top two photographs show poly films grown on Si and Ta substrates which had been pre-coated, respectively, with thin evaporated films of Au and Sn. It is obvious, by comparison with Fig. 13, that much larger grains (up to ~ 10 μm) were produced, very likely by some variant of the VLS mechanism;[11] but the size distribution is very non-uniform in the Au/Si case and the film is discontinuous in the Sn/Ta case. Moreover, incorporation of large amounts of Au into the GaAs would probably be deleterious to carrier

lifetime in solar cells. The picture labeled "Heat Treat" shows grain growth in a film originally deposited on graphite and looking much like the films of Fig. 13. The heat treatment consisted of heating four hours at 1050°C in a sealed tube containing As vapor and produced large, rounded grains but also a discontinuous surface. In the vitreous C example there was no special treatment, but the grain size increased appreciably nonetheless. Since, however, this result was not reproducible, it is believed to be due to impurities in the vitreous C which bring about an effect similar to that in the top two photographs of Fig. 14.

All the previously described experiments were carried out at 700°C and approximately the same flow rates. At this juncture, it was decided to vary these parameters. Figure 15 shows that an increase of supersaturation (flux of $Ga(CH_3)_3$) at 700°C has no effect. However, a significant increase in crystallite size is effected by going to an 850°C growth temperature, albeit at the expense of greatly reduced nuclei density leading to incomplete coverage. The density of nuclei is increased somewhat at higher supersaturations, although the grain size remains about the same.

A two-step growth procedure based on the foregoing findings has recently yielded our best results to date. By nucleating the film at 600°C for 15 seconds and then raising the temperature to 850°C and continuing the growth for 15 minutes, an approximately 6 μm thick film consisting quite uniformly of 2 to 3 μm grains was obtained. Although not spectacular, the device properties obtained with this film are our best so far. Parameters measured for a 100 Å Au Schottky barrier device with no AR coating and AM0 illumination are: V_{oc}=371mv; J_{sc}=15.7ma/cm^2; FF=.28; η=1.28%. Note that J_{sc} for this device is about 72% of what it would be for a single crystal device, in good agreement with the prediction of Fig. 3 of Ref. 6.

TABLE 1

Effects of Annealing on Solar Cell Behavior.

500 Å Pd + 5000 Å Al Contacts, No A.R. Coating.

10′ Anneals in N_2-H_2.

AM0 Illumination.

Device	Anneal Temp, °C	R_{Series} (ohms)	V_{oc} (volts)	FF	J_{sc} (mA/cm^2)	I(−1 volt) (amp)
SCL91	None	55	1.019	.45	22.2	$3x10^{-9}$
(Area=	225	50	1.015	.46	22.2	$3x10^{-9}$
0.5cm^2)	250	16	1.020	.64	23	$3x10^{-9}$
	275	6.5	1.022	.70	24	$3x10^{-9}$
	275(30′)	18	1.011	.64	22.2	$9.5x10^{-8}$
	300	6	0.843	--	22	$8x10^{-7}$
SCL82-1	None	26	0.990	.716	21.8	$2.6x10^{-9}$
	233	10	0.989	--	22.7	$17x10^{-9}$
	250	9	0.870	--	22.6	$5.1x10^{-6}$

TABLE 2

Device Properties at AM0, 30°C,

Power Input = 134.8 mW/cm^2.

Device	V_{oc} (volt)	J_{sc} (mA/cm^2)	FF	R_{Series} (ohm)	η %
81-1	1.015	33.1	.745	9	18.5
81-3	0.998	32.1	.771	4.6	18.3
83	1.019	30.3	.702	6.0	16.1
84-2	0.985	29.1	.751	4.0	16.0
85-1	0.978	25.5	.52	70	9.6
91	1.022	31.2	.70	6.5	16.6
101A	1.004	30.7	.795	4.4	18.1
115	0.991	30.5	.803	1.7	18.0

References

1. Hovel, H. J.: and Woodall, J. M.: Optimization of Solar Cells for Air Mass Zero Operation and a Study of Solar Cells at High Temperatures, Final Report, Phase I. NASA Contract NASI-12812, March 1975.

2. Hovel, H. J.; and Woodall, J. M.: Technique for Producing "Good" GaAs Solar Cells Using Poor Quality Substrates. Appl. Phys. Lett., vol. 27, 1975, pp. 447.

3. Fitzgibbons, E. T.; Sladek, K. J.; and Hartwig, W. H.: TiO_2 Film Properties as a Function of Processing Temperature. J. Electrochem. Soc., vol. 119, 1972, pp. 735.

4. Hovel, H. J.; and Woodall, J. M.: Optimization of Solar Cells for Air Mass Zero Operation and a Study of Solar Cells at High Temperatures, Final Report, Phase II. NASA Contract NASI-12812, March 1, 1976.

5. Woodall, J. M.; and Hovel, H. J.: Outlooks for GaAs Terrestrial Photovoltaics. J. Vac. Sci. Technol., vol. 12, 1975, pp. 1000.

6. Lanza, C.; and Hovel, H. J.: Efficiency Calculations for Thin-Film Polycrystalline Semiconductor Schottky Barrier Solar Cells. Conf. Rec. 12th IEEE Photo. Spec. Conf., Baton Rouge, Nov. 1976, IEEE Trans. El. Dev. Vol. ED-24, 1977, pp. 392.

7. Vohl, P.; Perkins, D. M.; Ellis, S. G.; Addiss, R. R.; Hui, W.; and Noel, G.: GaAs Thin Film Solar Cells. IEEE Trans. Electron Devices, vol. 14, 1967, pp. 26.

8. Manasevit, H. M.; and Simpson, W. I.: The Use of Metal-Organics in the Preparation of Semiconductor Materials, I. Epitaxial Gallium-V Compounds. J. Electrochem. Soc., vol. 116, 1969, pp. 1725.

9. Bass, S. J.: Device Quality Epitaxial Gallium Arsenide Grown by the Metal Alkyl-Hydride Technique. J. Crystal Growth, vol. 31, 1975, pp. 172.

10. Amick, J. A.: The Growth of Single-Crystal Gallium Arsenide Layers on Germanium and Metallic Substrates. RCA Review, vol. 24, 1963, pp. 555.

11. Wagner, R. S.; and Ellis, W. C.: Vapor-Liquid-Solid Mechanism of Single Crystal Growth. Appl. Phys. Lett., vol. 4, 1964, pp. 89.

Figure Captions

Figure 1 Time-temperature growth schedule for etchback-regrowth epitaxy with excess GaAs. (1)Furnace upheat and equilibration; (2)isothermal equilibration of Ga-Al, Zn doped melt with GaAs; (3)upheat of melt, contact of GaAs substrate, with melt, etchback-regrowth step, and substrate removal from melt.

Figure 2 Time-temperature growth schedule for etchback-regrowth epitaxy with no excess GaAs. (1)Furnace upheat and equilibration; (2)contact of GaAs substrate with melt, etchback-regrowth step, and substrate removal from melt.

Figure 3 Spectral responses of cells grown at 870°C, showing the effect of leaching and Zn doping level. No AR coating.

Figure 4 Spectral responses of cells grown at 800°C. No AR coating.

Figure 5 Spectral responses of two cells with and without TiO_2 anti-reflective coating.

Figure 6 A comparison of the spectra of AM0 light and H_2O+I.R.filtered Xe light.

Figure 7 Photocurrent density versus temperature, indicating an initial rise followed by a slight decline.

Figure 8 Open circuit voltage as a function of temperature.

Figure 9 Efficiency for AM1.5 light and for simulated AMO light as a function of temperature.

Figure 10 Spectral response versus junction depth. Dotted line = calculated response for a 1000 Å junction depth.

Figure 11 Dark J-V curves for junction depths of 3000 Å (not anodized) and 500 Å. A

typical GaAlAs-GaAs cell is also shown.

Figure 12 Short circuit current and efficiency under simulated AM0 light. (No contact area correction).

Figure 13 SEM micrographs of polycrystalline GaAs deposits on three different metals.

Figure 14 SEM micrographs of deposits on variously-treated substrates.

Figure 15 Effect of varying the supersaturation and growth temperature on the grain morphology.

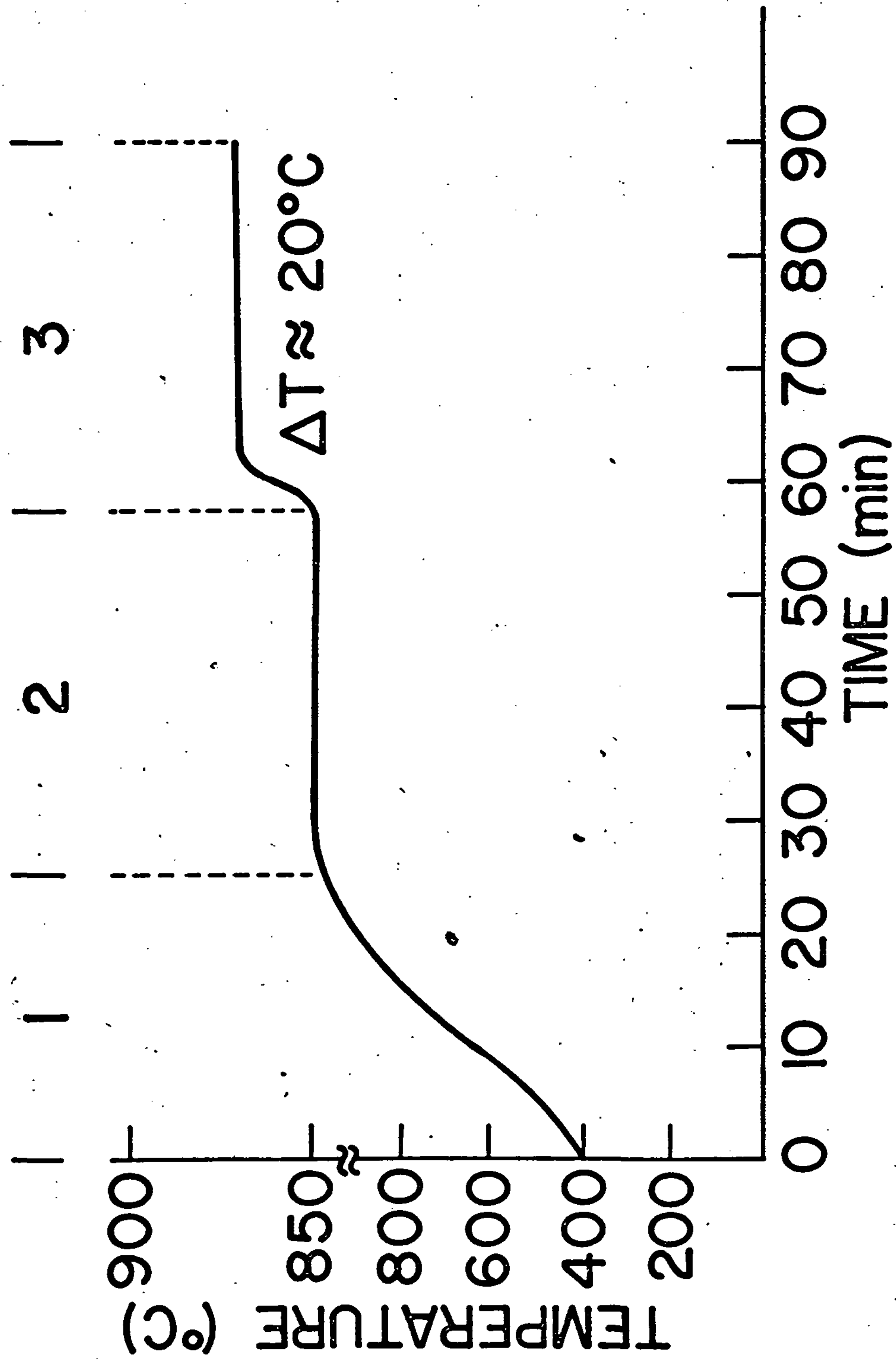

FIGURE 1

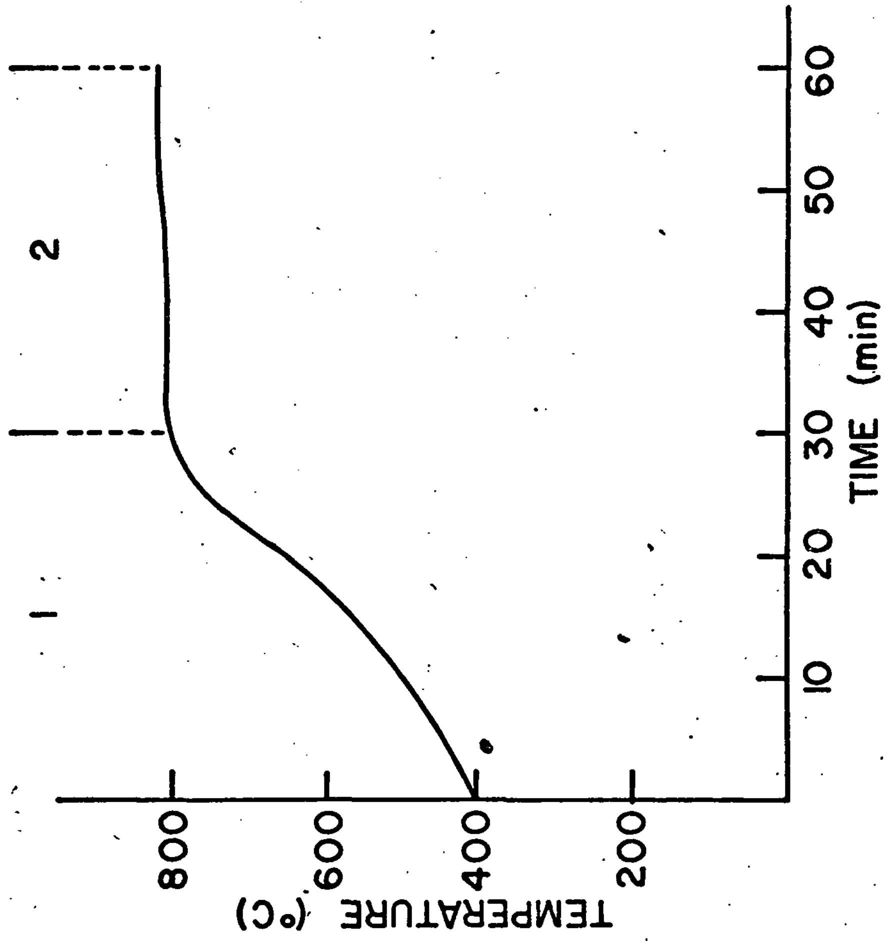

FIGURE 2

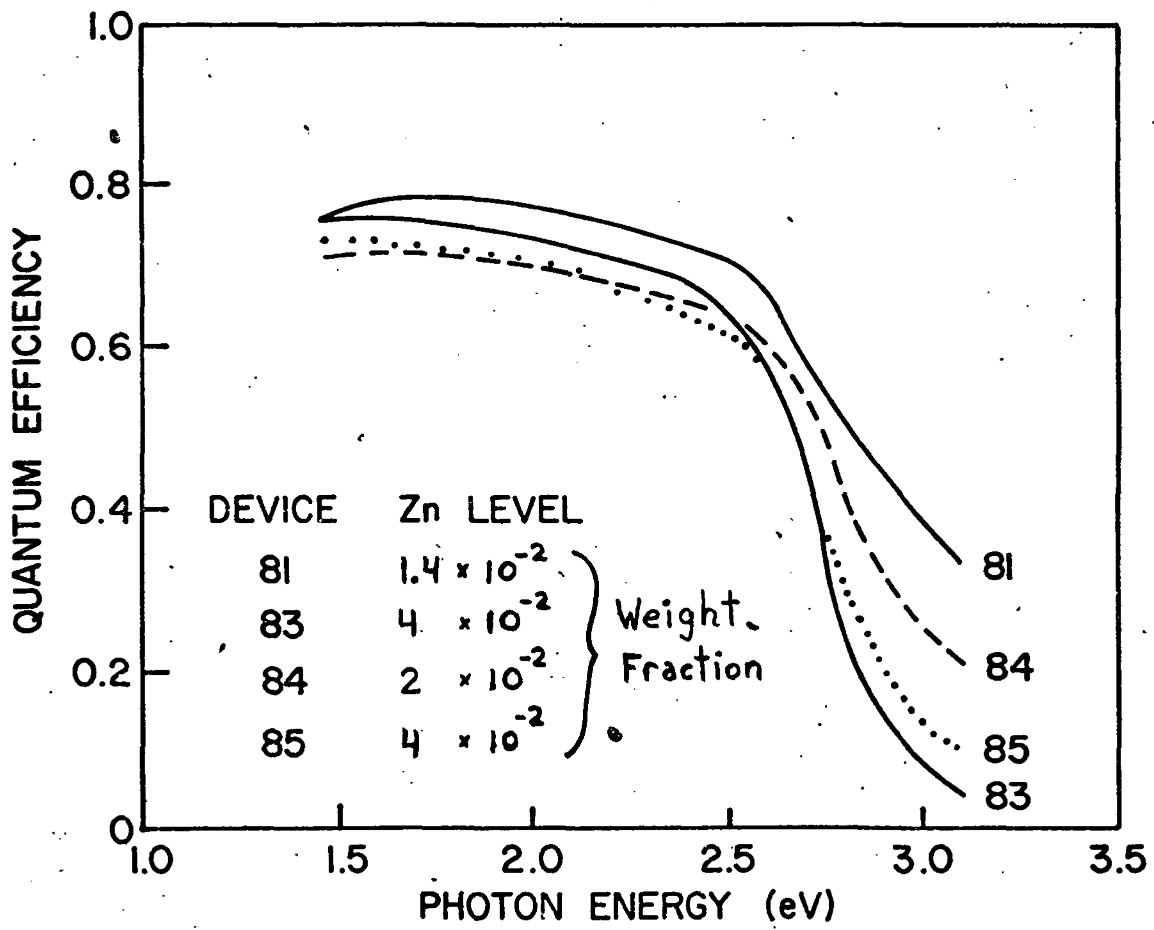

FIGURE 3

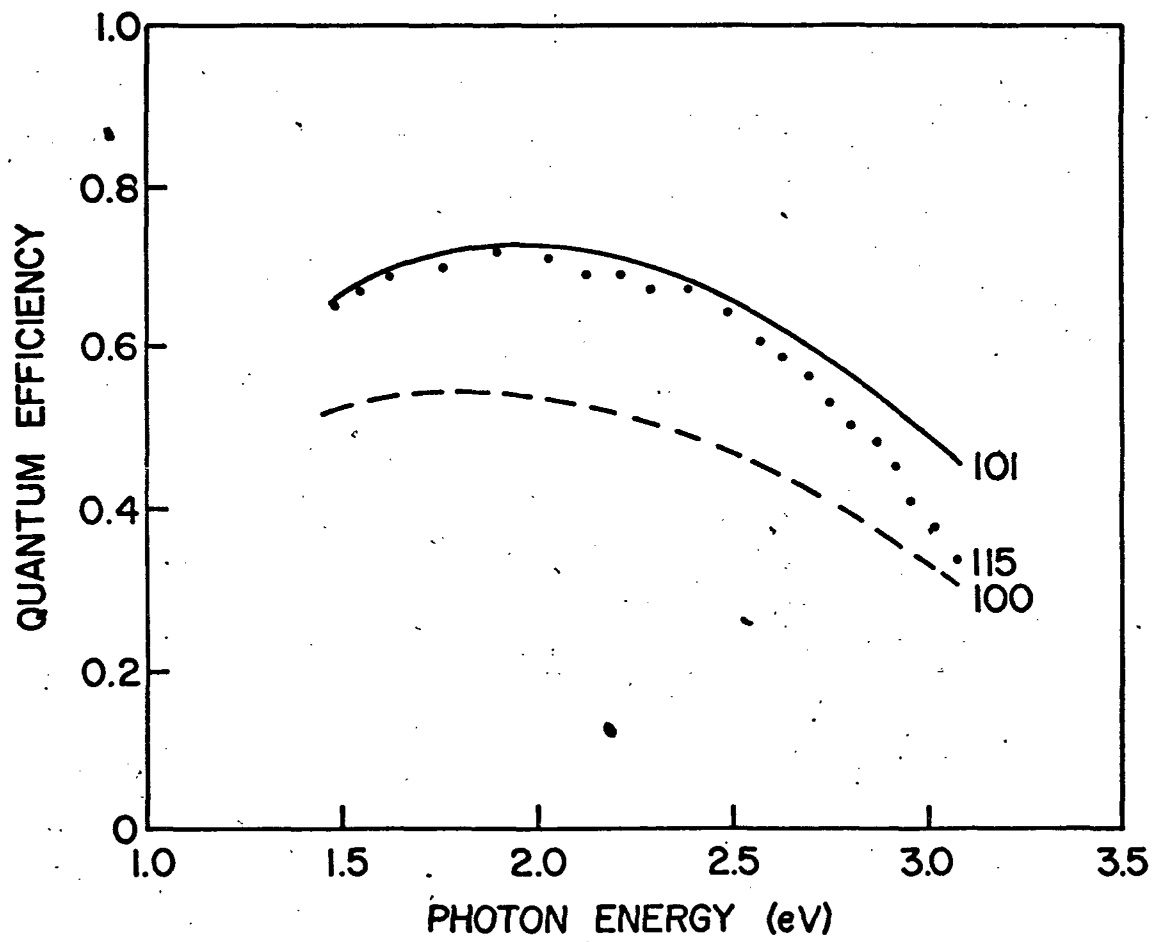

FIGURE 4

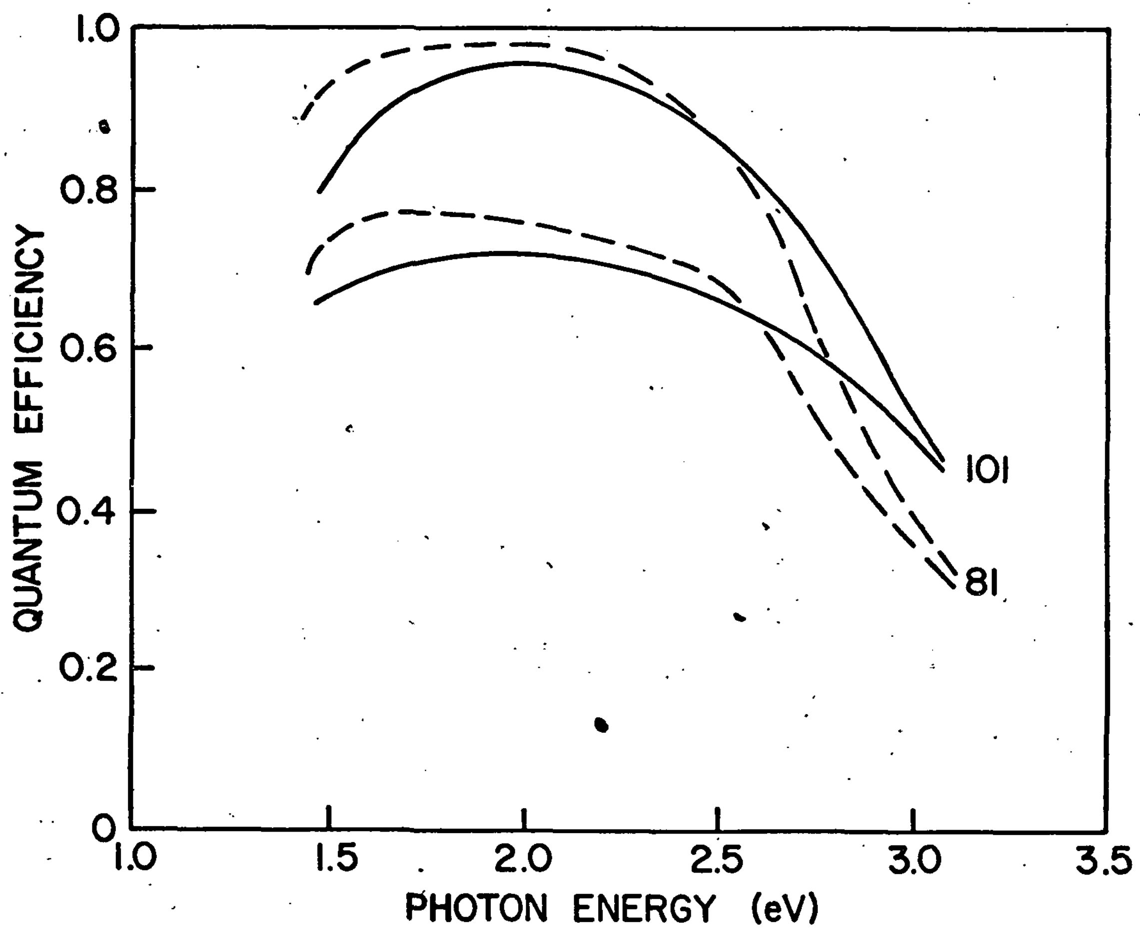

FIGURE 5

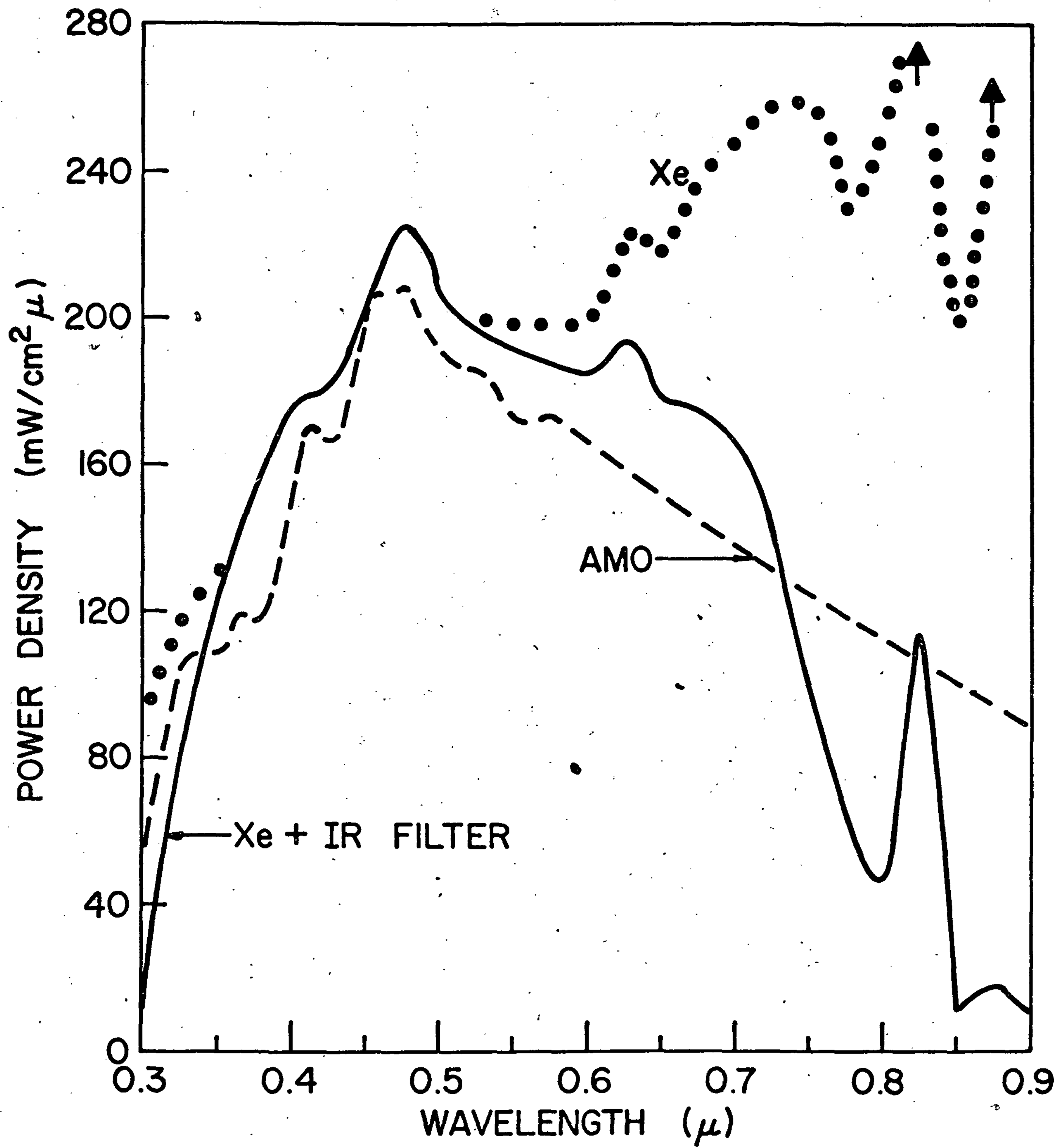

FIGURE 6

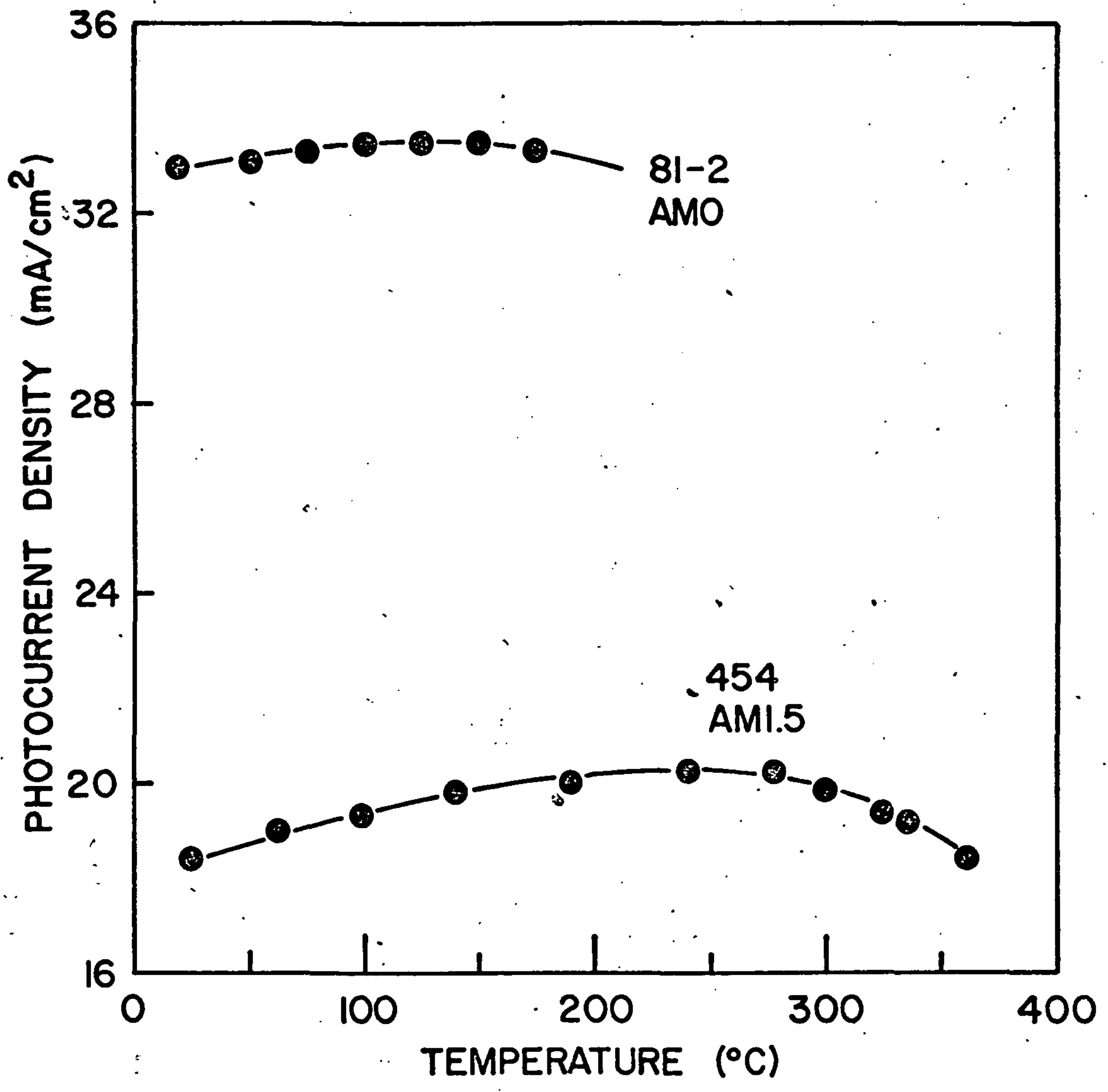

FIGURE 7

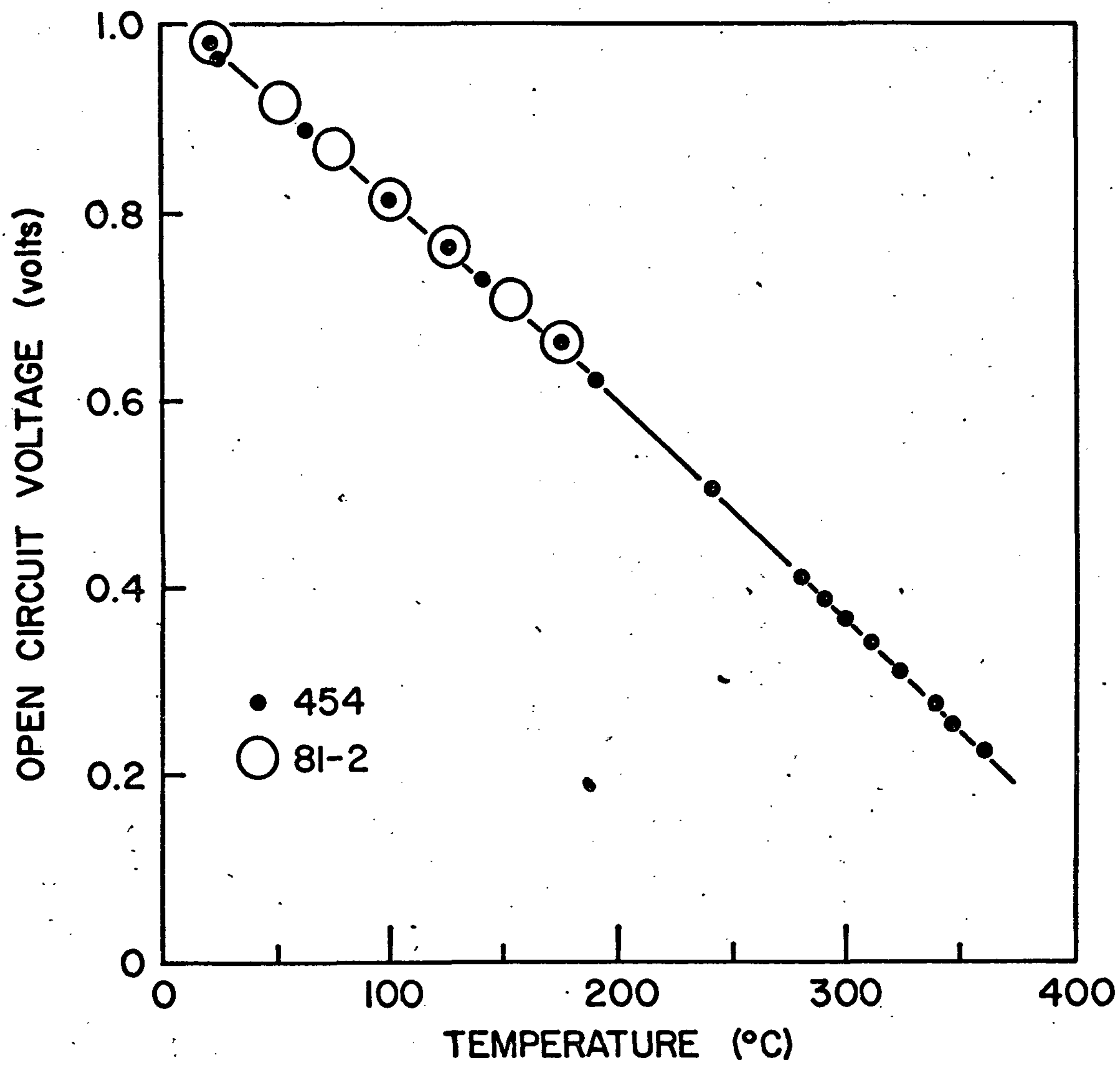

FIGURE 8

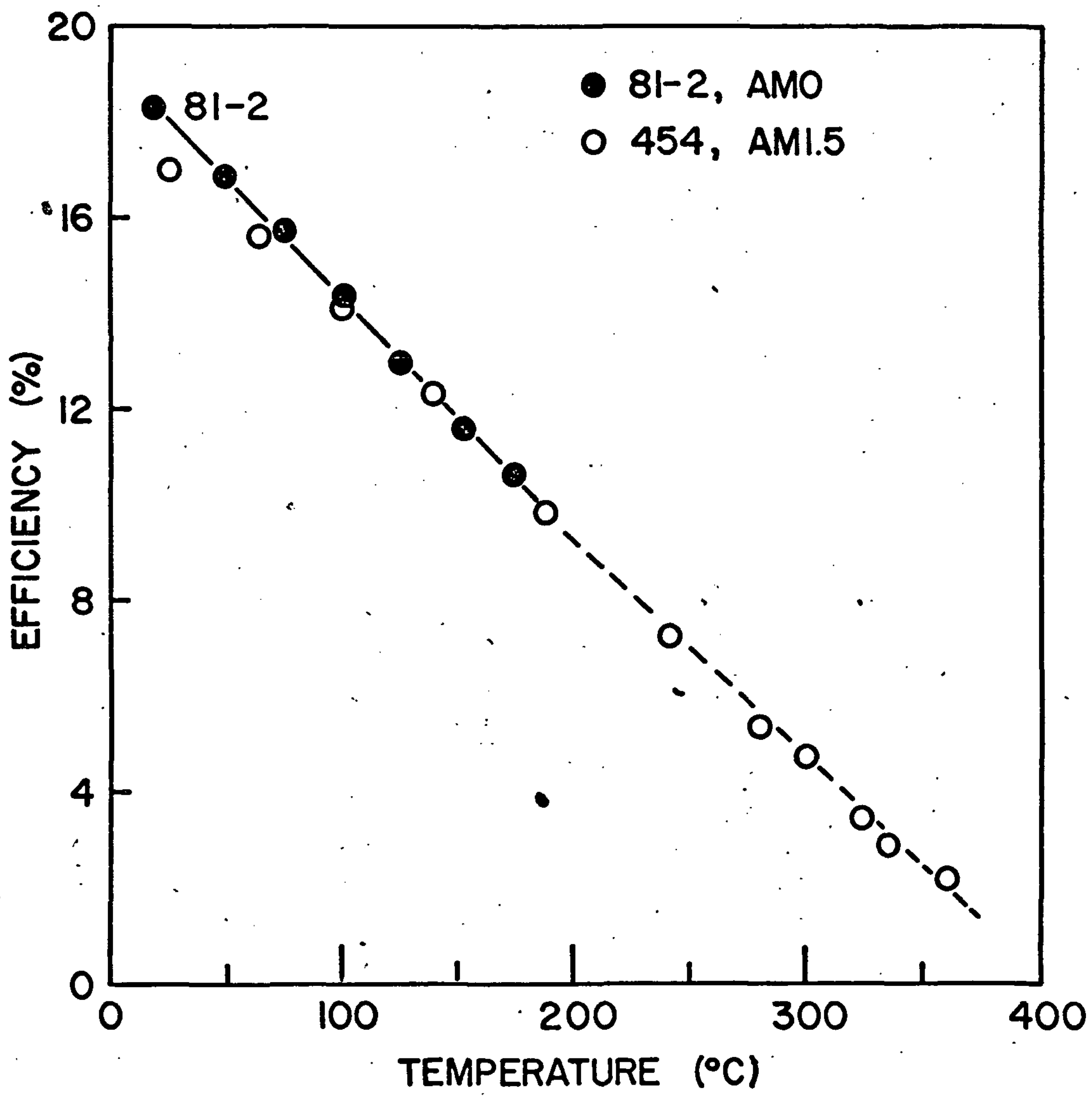

FIGURE 9

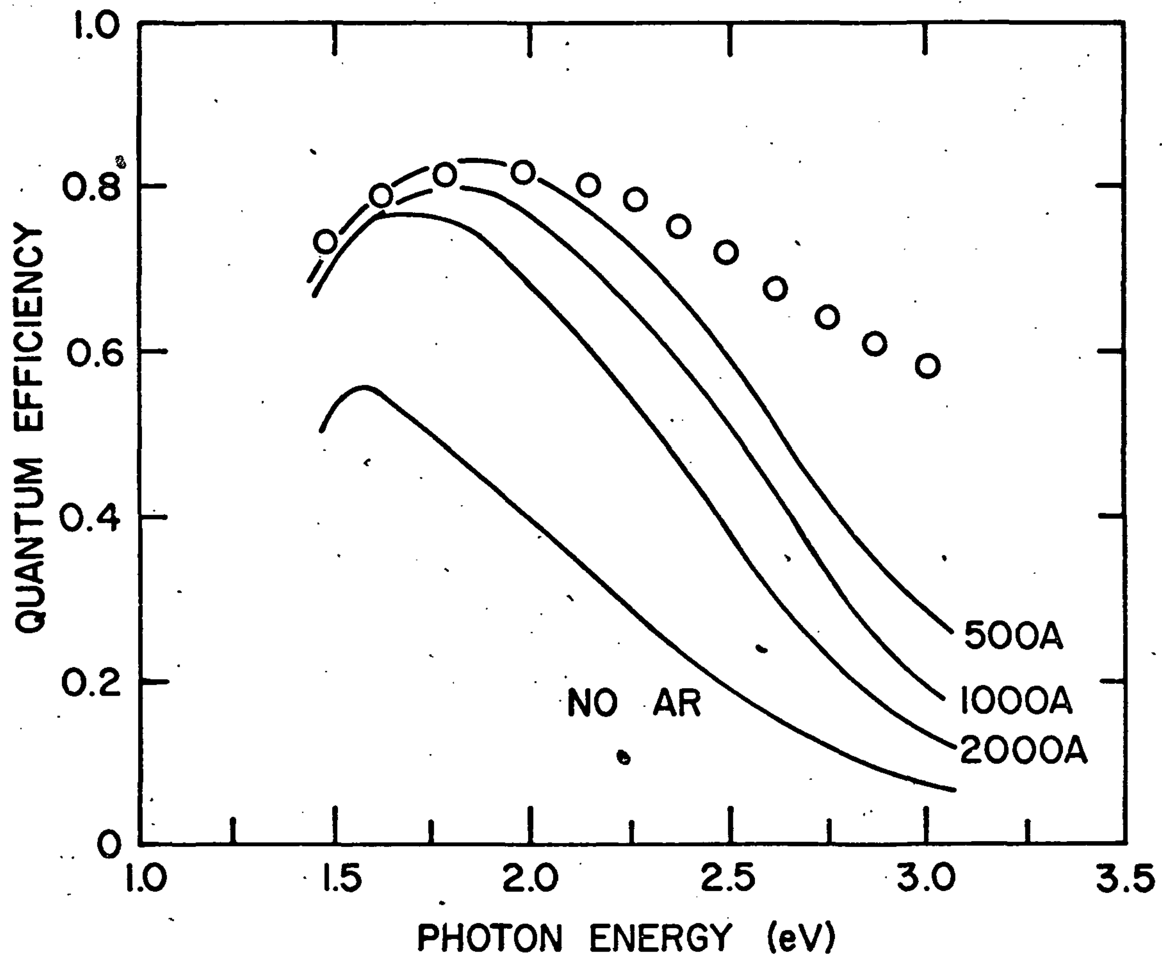

FIGURE 10

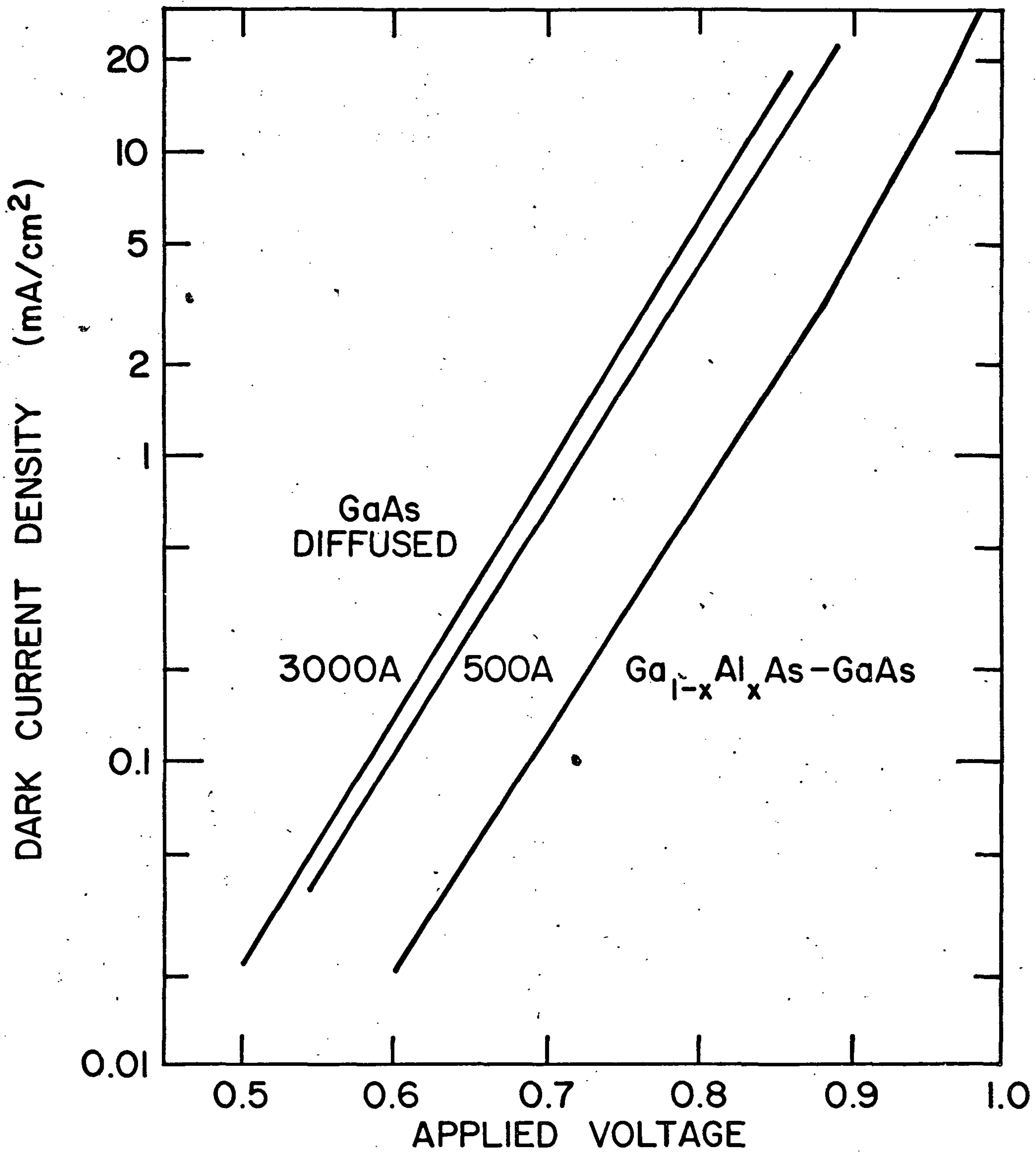

FIGURE 11

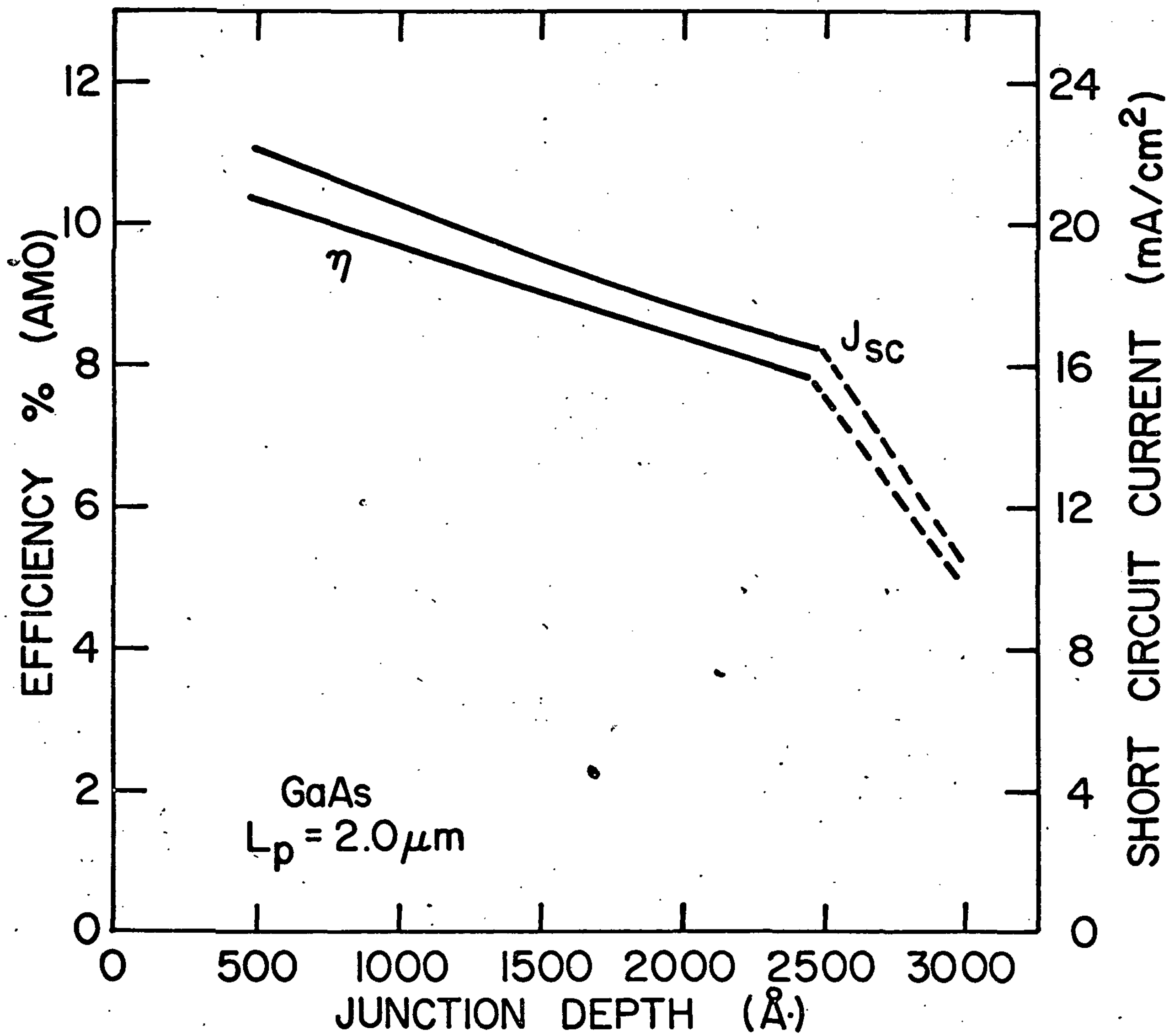

FIGURE 12

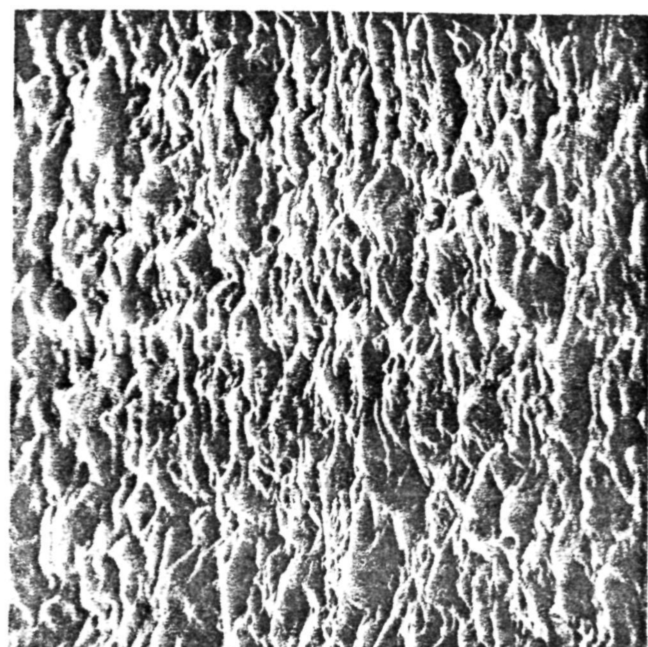

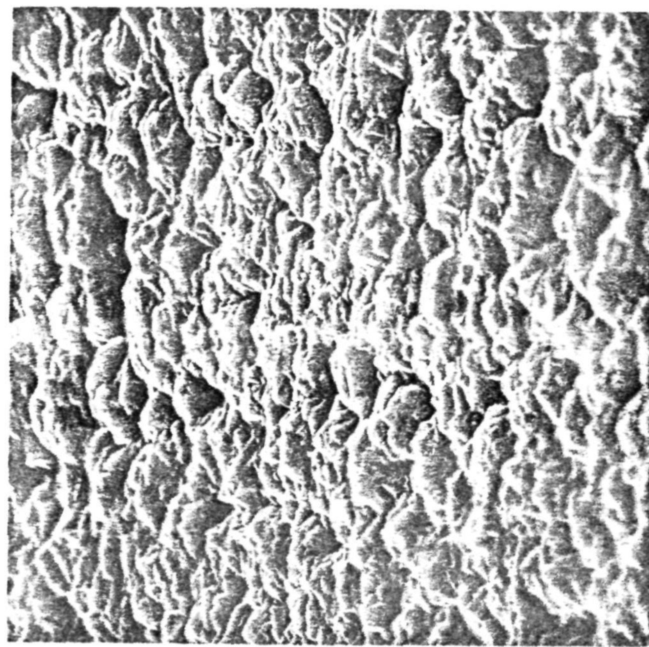

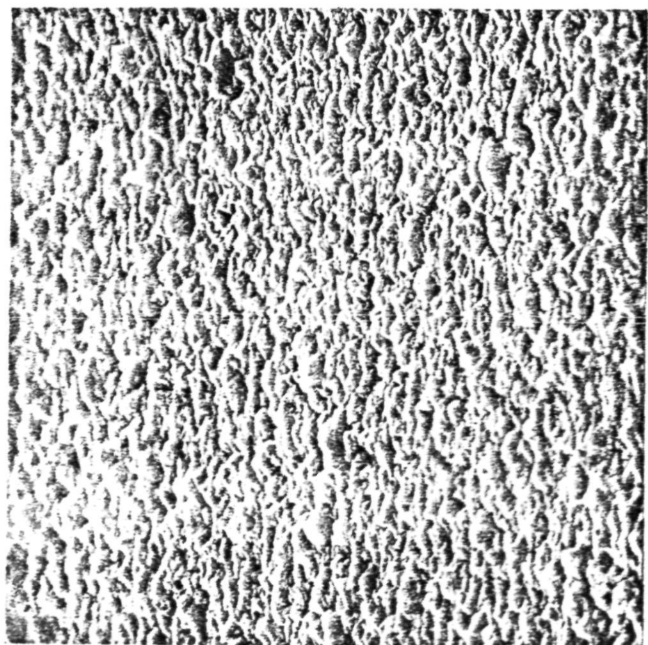

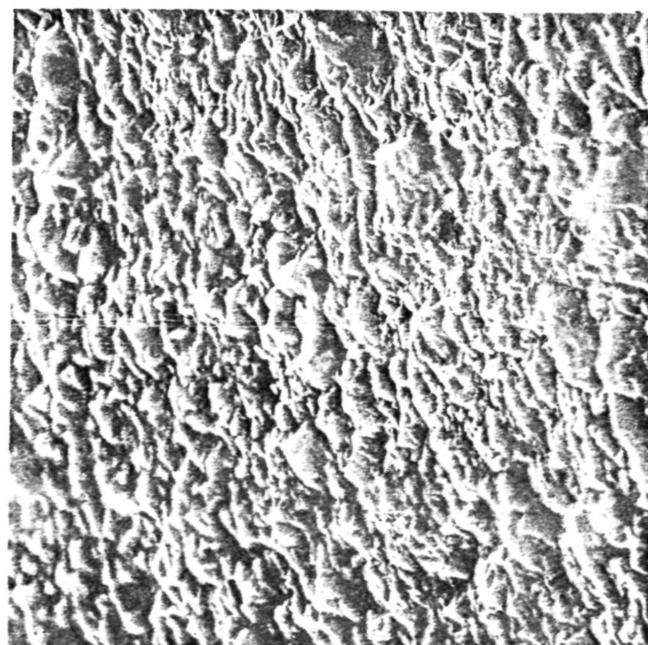

FIGURE 13

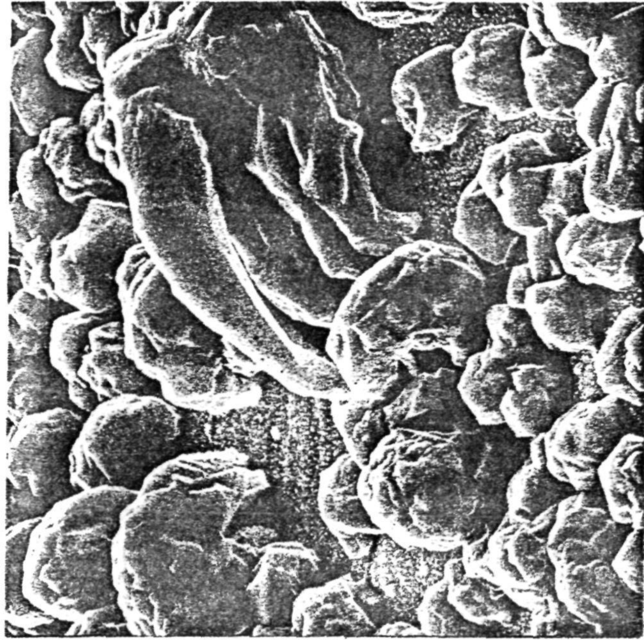

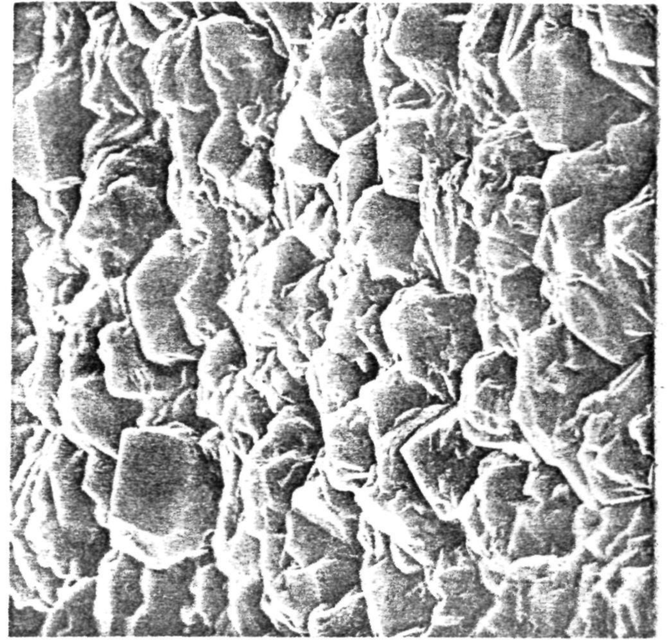

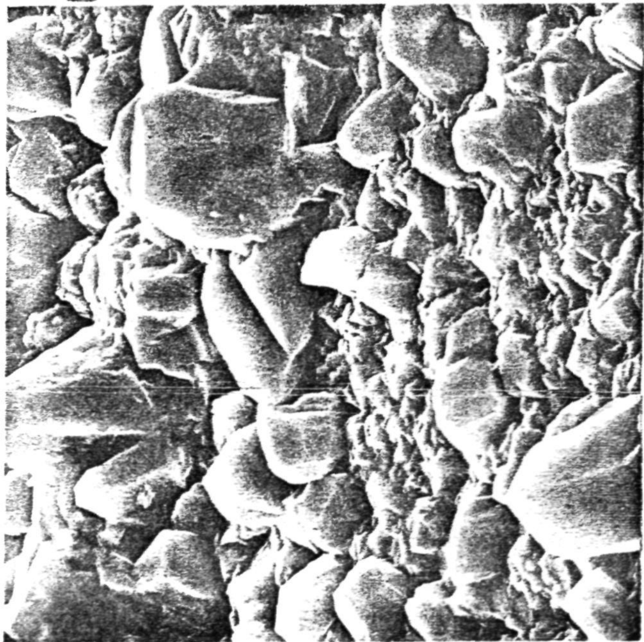

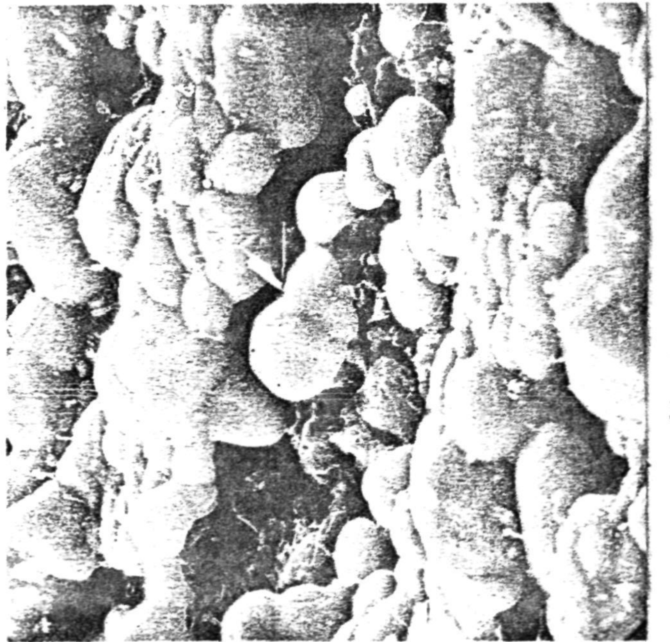

FIGURE 14

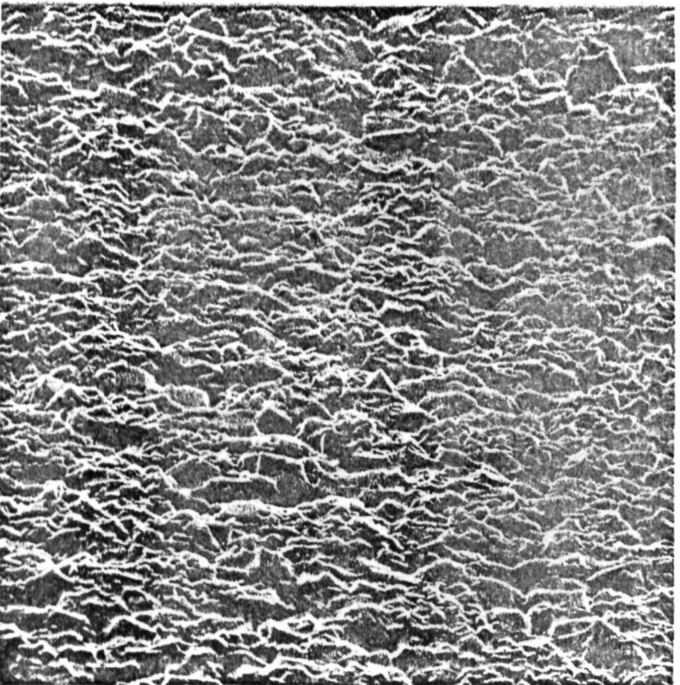
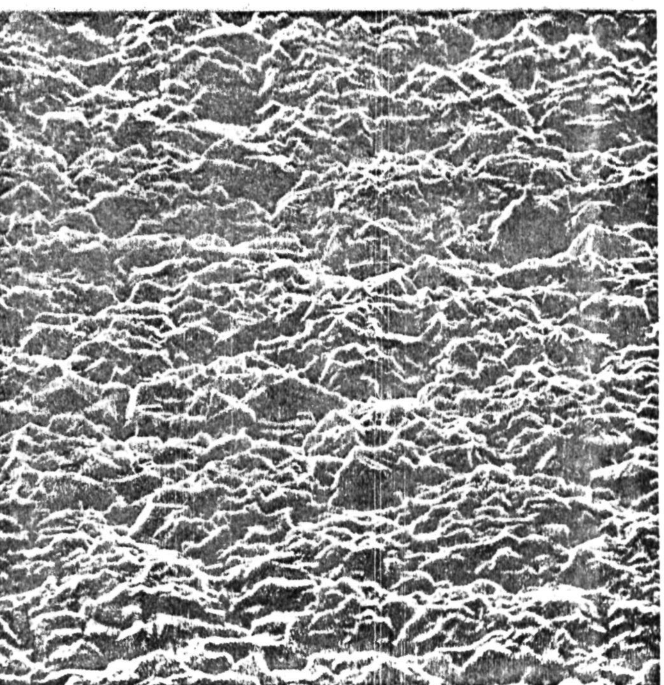
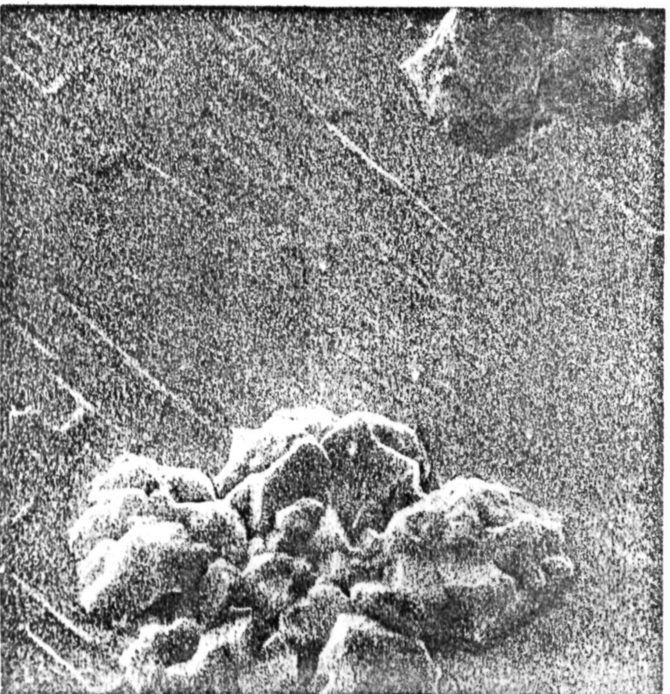
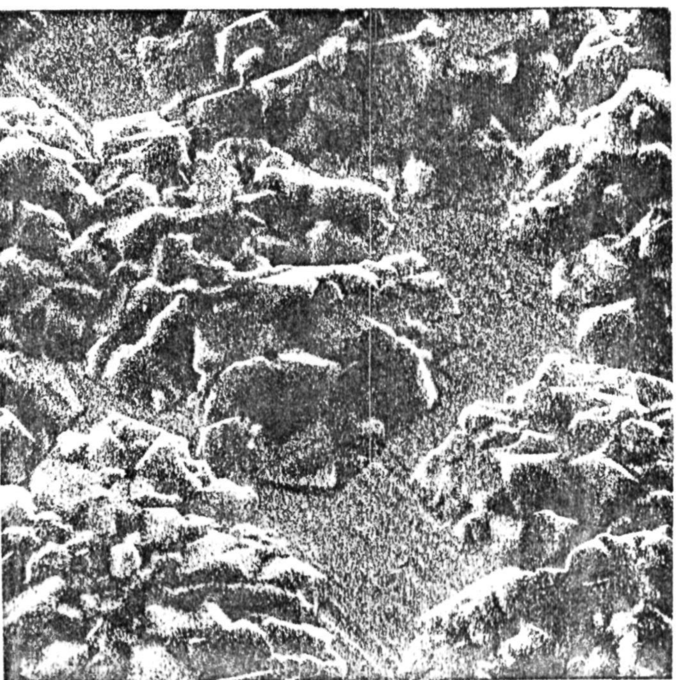

FIGURE 15